Liu, S., Pan, W., Zhao, X., Zhang, H., Cheng, X., Long, Z., and Chen, Q. 2018. "Influence of surrounding buildings on wind flow around a building predicted by CFD simulations," *Building and Environment*, 140: 1-10.

Influence of surrounding buildings on wind flow around a building predicted by CFD simulations

Sumei Liu[a], Wuxuan Pan[a], Xingwang Zhao[a], Hao Zhang[a], Xionglei Cheng[a], Zhengwei Long[a,*], Qingyan Chen[b,a]

[a]*Tianjin Key Laboratory of Indoor Air Environmental Quality Control, School of Environmental Science and Engineering, Tianjin University, Tianjin, China*

[b]*School of Mechanical Engineering, Purdue University, West Lafayette, IN, USA*

HIGHLIGHTS

- Simulation of intermediate terrain between an urban configuration and a meteorological station with the use of roughness length.
- Study of minimum number of surrounding buildings to be included when simulating wind flow around a target building.
- Verification of the simulation results with measured wind velocity on building rooftops.
- Examination of the use of these approaches for different wind directions.

ABSTRACT

This investigation used wind information from a meteorological station to conduct a CFD study of wind distribution in an urban configuration. The study treated the computational domain with detailed building structures only in the proximity of the urban configuration, and treated other regions with roughness. The resulting mean wind velocity was 5.5% higher than that computed with the use of detailed building structures between the meteorological station and the urban configuration, which is acceptable for most applications. This investigation then explored the influence of surrounding buildings on the wind flow around the target building with different geometrical models. The models differed in terms of the geometrical details around the building. The results showed that the surrounding buildings had a considerable impact on the wind flow around the target building due to the sheltering and channeling effect. When the details of the surrounding building structures were not taken into account, the wind flow around the building was inaccurate and unacceptable. The predicted wind speed and pressure distributions improved with an increase in the level of detail of the surrounding building structures. To achieve acceptable results, a CFD simulation should use detailed building structures around the target building within a radius of at least three times the length scale, where the length scale is the largest dimension of the target building. The results of the study can serve as a practical guide for predicting airflow around an urban configuration or a building.

Keywords: Urban wind flow, Geometric model, Surface roughness, Experimental verification

1. Introduction

The investigation of wind around buildings in an urban configuration in the lower part of the atmospheric boundary layer (0-200 m) [1] is crucial in many wind environmental problems, including natural ventilation design, pedestrian comfort, and air pollutant dispersion [2, 3]. Solving wind-environment problems requires the study of wind flow into an urban configuration [4, 5]. With the development of computing resources and grid-generation techniques, an increasing number of researchers have adopted computational fluid dynamics

(CFD) in their investigation of urban wind environments [6-9]. The accuracy of CFD simulations relies on many factors, and to the knowledge of the authors, computational domain and representation of surroundings are the prerequisite to acquire accurate results [10].

Traditional CFD models for urban flow simulation can be classified as meso-scale models (10 to 200 km in the horizontal direction) and micro-scale models (100 m to 2 km in the horizontal direction) [11,12]. Meso-scale models do not provide detailed flow information below the urban canopy layer. Because these models use parametrization methods for the building details, the results are not useful for designing natural ventilation in buildings, pedestrian comfort, or air-pollutant dispersion [13,14]. Micro-scale models use meteorological data from several kilometer away as the inflow boundary and do not explicitly consider the effect of the distance from the meteorological station to the urban configuration. Thus, the simulated wind environment may not be accurate [15,16]. We [17] previously proposed a full-scale model (typically 2 to 20 km long) that is a cross between a micro-scale and a meso-scale model. The full-scale model is similar to a micro-scale model in that the building details are explicitly constructed; however, the computational domain extends from the urban configuration site to a meteorological station several kilometer away. The full-scale model was able to produce the wind velocity distribution in the urban configuration with the use of wind information from a meteorological station 10 km away from the urban configuration. Although the full-scale model calculated the wind distribution at the urban configuration site with reasonable accuracy, constructing all the building details in the computational domain was very time consuming, and the computation required significant computing resources.

In fact, we are concerned only with the flow distribution inside a particular urban configuration. Therefore, it would be more practical to only construct building details inside the urban configuration area, while treating the terrain between the urban configuration and the meteorological station as some kinds of resistance. The question now is how to manipulate the urban architecture between the urban configuration and the meteorological station. Meso-scale models generally use parametrization methods for building details in order to emphasize the impact of geographical and meteorological conditions on urban wind environments [18]. These parametrization methods can be classified into three categories, drag force parametrization [19-21], porosity concepts [22-24] and roughness length approaches [25-27]. The drag force parametrization and porosity concepts use wind tunnel experimental data in which roughness elements are simple cubes with given distributions, whereas actual urban constructions are highly spatially inhomogeneous; thus, the methods may not be suitable for an actual urban environment. The roughness length method is a very simple way to include the effects of urban terrain on wind speed and turbulence by using a prescribed aerodynamic roughness z_0 in contrast to the urban terrain, which is of great importance in building and wind engineering applications. However, the performance of the method in representing building structures in an actual urban area for the purpose of urban flow simulation has not been thoroughly evaluated.

In addition to the unresolved issue of representation of the intermediate terrain, another problem is the size of the region in which building details should be explicitly constructed. In an urban area, the wind flow around a building is often influenced by surrounding buildings because of the buffeting, channeling, and sheltering effects [28, 29]. van Hooff and Blocken [30] observed that the ACH (air change rate per hour) in a building was highly dependent on the surrounding buildings. Excluding the urban environment in the computational domain can lead to an overestimation of the ACH. Therefore, to ensure accurate results, it is important to construct a reasonable representation of the surroundings in the CFD simulations. Tominaga et al. [10] suggested the modelling of surrounding buildings within a 1H-2H radius from the

target building, where H is the height of the target building. Moreover, at least one additional street block in each direction around the assessment region should also be clearly reproduced. Tong et al. [31] recommended that three layers of buildings in the surroundings (n = 3) be modelled explicitly for regular street canyons (H/W = 1, where H is the height of the building on the street side, and W is the width of the street) under normal and oblique wind directions, while reducing the influence region to two layers (n = 2) for wide canyons (H/W = 1/3) and a high-rise configuration. However, previous studies were based on simple cubes with given distributions, whereas the actual building structures in an urban area are extremely complex. It was also difficult to define surrounding layers on the basis of building blocks, because buildings could be distributed densely in some directions but sparsely in the other directions.

Previous studies have not determined how to correctly represent the urban architecture between the urban configuration and the meteorological station, or how many of the buildings around a target building should be explicitly constructed in a real urban area. This investigation examined the use of roughness length to simulate the intermediate terrain, in order to identify a suitable method for accurately calculating the wind distribution in an urban configuration with limited computing resources. Using the proposed method, this investigation then compared simulations with different surrounding layers and a simplified geometric model. The aim was to reduce the effort in constructing the geometric model with the inclusion of building details and to reduce computing costs, while maintaining the accuracy of the simulated wind flow at an acceptable level.

2. Research Method

This section describes the construction of a geometric model to represent the region between an urban configuration and a meteorological station; the numerical model that was used to compute the wind distribution in the region; the construction of the mesh grid for the computational domain; the boundary conditions that were used; and the experimental procedure for obtaining wind information to validate the numerical results.

2.1 Geometric model

This investigation first explored the feasibility of simulating the intermediate terrain with the use of roughness length. We used a detailed full-scale geometric model that extended from an urban configuration (Tianjin University) to the nearest meteorological station (Xiqing station), 10 km away in Tianjin, China. The computational domain was 12.6 km long, 5.4 km wide and 0.351 km high, as shown in Fig. 1(a). The model divided the computational domain into three regions: the center region included geometrical details of the buildings between the urban configuration and the meteorological station, and the buildings on both sides were represented by roughness lengths. More detailed information can be found in Liu et al. [17].

For comparison, this study also constructed a simplified full-scale model as shown in Fig. 1(b). The computational domain of this model was the same as that of the detailed full-scale model, but only the building structures in the urban configuration site concerned (enclosed by the white box in the figure) were explicitly constructed, as shown in Fig. 1(c), while other regions were simplified with roughness length. With the use of a satellite map, the computational domain was partitioned into regions of different roughness length according to building density and building height. Evaluation of these two cases allowed us to identify a suitable method of simulating the intermediate terrain with roughness length in order to accurately calculate the wind distribution in an urban configuration with limited computing resources.

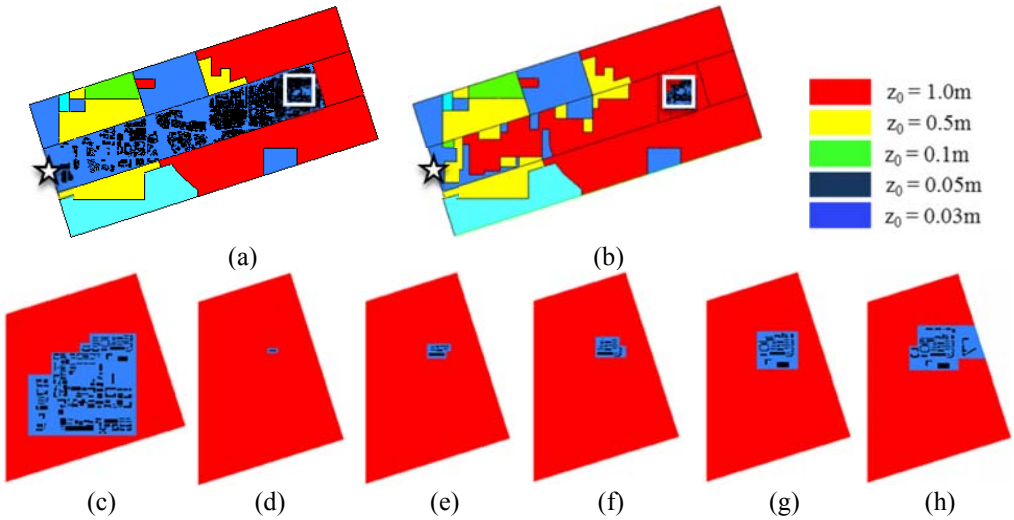

Fig. 1. Geometric models used in this study: (a) a detailed full-scale geometric model with building structures for the entire computational domain from an urban configuration (indicated by the white box) to the nearest meteorological station (indicated by the star), (b) a simplified full-scale model with detailed building structures inside the urban configuration and roughness lengths for the rest of the computational domain; (c) the building structures of the Tianjin University (TJU) model, (d) a single target building (R = 0), (e) with R = L surroundings, (f) with R = 2L surroundings, (g) with R = 3L surroundings, and (h) with R = 4L surroundings.

Using the simplified method, we then explored the influence of surrounding buildings on the wind flow around a target building. The target building was a residential building inside the urban configuration; it was 65 m long, 15 m wide and 16 m high, as shown in red on the map in Fig. 2. This investigation chose the maximum dimension of the building, i.e., the length (L = 65 m), as a scale in the radial direction in order to take into account surrounding buildings at various distances from the target building. Different layers were defined as multiples of the scale. Whenever more than 50% of the area of a surrounding building fell within a given multiple of the radius, it was included in that layer. Fig. 2 shows buildings in five different layers used in this investigation. Fig. 1(d) depicts the layer with only the target building (R = 0), Fig. 1(e) the layer with R = L buildings, Fig. 1(f) with R = 2L buildings, Fig. 1(g) with R = 3L buildings, and Fig. 1(h) with R = 4L buildings. The area outside the detailed building structures can be simulated by a roughness length corresponding to the building area. By comparing with the simplified full-scale model, this investigation explored the influence of different layers around the target building.

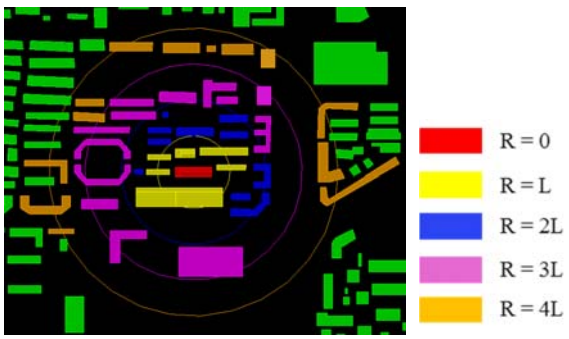

Fig. 2. Multiple layers of the surroundings defined for the target building.

Because of the complexity of the building structures around the target building in different directions, it was important to perform simulations for other wind directions to confirm the influence region of the surroundings. For this purpose, we selected the Beichen station and the Dongli station, as shown in Fig. 3(a). The two stations were located 14.3 km from the campus in the north-north-west (NNW) direction and 15.1 km from the campus in the east-south-east (ESE) direction, respectively [32]. Following the same method as was used for the model shown in Fig. 1(b), Figs. 3(b) and 3(c) depict the corresponding simplified full-scale models for the two meteorological stations. Again, this study constructed another five simplified models (with surrounding buildings from R = 0 to R = 4L) for the Beichen and Dongli stations.

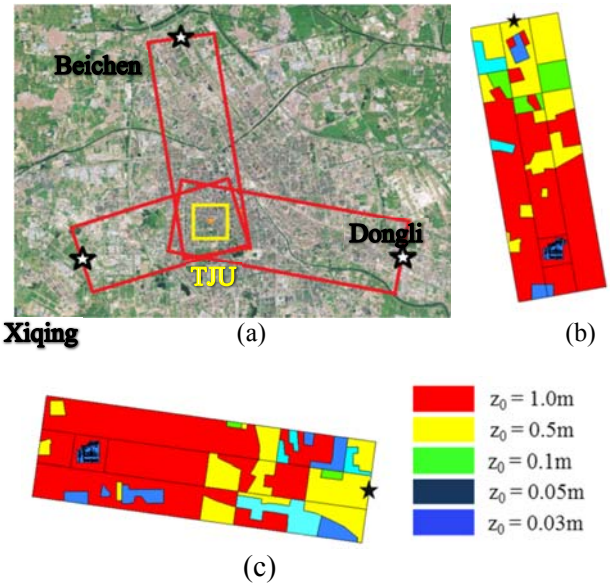

Fig. 3. (a) Relative locations of three meteorological stations around the Tianjin University campus (TJU) and computational domains of the other two simplified full-scale models: (b) Beichen model and (c) Dongli model.

2.2 CFD model

Our CFD simulations utilized a commercial program, ANSYS Fluent 14.0 [33]. The simulations used the Reynolds-averaged Navier-Stokes (RANS) equations with a realizable k-ε turbulence model [34] to solve the turbulent wind flow in the computational domain. The model performed well in simulating urban wind flows with an average relative error of 12% compared with the measured data [35]. The governing transport equations were solved by means of the finite volume method. The SIMPLE algorithm was used for pressure and velocity coupling of the transport equations, and second-order discretization schemes were used for solving all the independent variables. When the scaled residuals reached 10^{-4} for mass conservation, U, V, W, k, ε, the solution was considered to be converged. Velocity magnitude on several specified points were also monitored to confirm that the solution did not change with the iteration, which was another criterion for convergence. For more detailed information about the numerical technique, please refer to the program manual [33].

2.3 Grid arrangement and mesh generation

Gambit 2.4.6 was used to generate a discrete grid for discretizing the governing transport equations. Because of the complexity of the geometric models, this study used a hybrid grid scheme with a tetrahedral grid, which was easily adapted to the geometric structures. The maximum grid size was 20 m near the meteorological station, and it was gradually reduced to 7 m at the urban configuration site in the lengthwise direction. The maximum grid size in the

vertical direction was 10 m. The grid resolution along the perimeter without buildings was 20 m. For the building structures around the target building, the grid size was refined to 1 m. This led to a total grid number of 8.9 million for the detailed full-scale model shown in Fig. 1(a). The mesh type for the simplified full-scale model was the same as that for the detailed full-scale model. Because roughness length was used in place of the detailed building structures between the urban configuration and the meteorological station, the total grid number was reduced to 6.1 million for the simplified full-scale models shown in Fig. 1(b) and Fig. 1(c). With the same method, the grid mesh sizes were 4.7 million, 4.7 million, 4.5 million, 4.4 million and 4.2 million cells for the models shown in Figs. 1(d) to 1(h), respectively. The grid number for the models with the other two meteorological stations was slightly higher because the stations were further away from the university campus. Fig. 4 shows the grid cells on the building surfaces and in the perimeter zone for the R = 4L models.

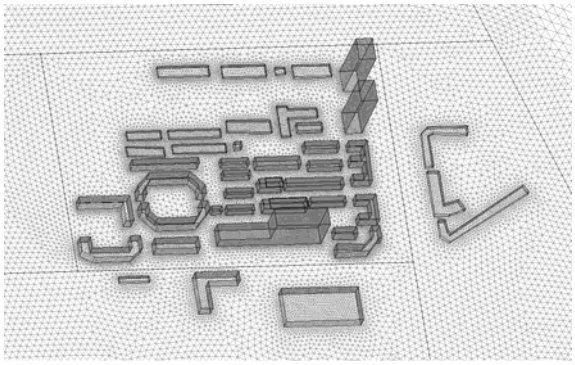

Fig. 4. Grid distribution on the building surfaces and in the perimeter zone for the R = 4L models.

2.4 Boundary conditions

The simulations used wind data from the meteorological station in the upwind direction as the inflow boundary conditions. Table 1 lists the selected data for the three meteorological stations. The upstream vertical boundaries (western and southern boundaries for the Xiqing model; northern and western boundaries for the Beichen model; and eastern and southern boundaries for the Dongli model) in the computational domain were set as inflow. The vertical velocity profile for the inflow boundary was modeled as a power law, and the vertical profiles for k_z and ε_z was taking from Richards and Hoxey [36].

$$U_z = U_r \left(\frac{z}{z_r}\right)^{\alpha} \tag{1}$$

$$k_z = U_{ABL}^{*2} \Big/ \sqrt{C_\mu} \tag{2}$$

$$\varepsilon_z = U_{ABL}^{*3} / k(z + z_0) \tag{3}$$

where U_r (m/s) is the velocity at reference height z_r (m), and z (m) is height. Because the meteorological station was located in a suburb, the exponent in the power law was $\alpha = 0.22$ [37] at the two inlet boundaries. k is the Karman constant (= 0.4) and $U_{ABL}^{*}$is the atmospheric boundary layer friction velocity. U_{ABL}^{*} is calculated from the velocity U_r (m/s) at reference height z_r (m) as

$$U_{ABL}^{*} = kU_r / \ln((h + z_0)/z_0) \tag{4}$$

The corresponding two downstream vertical boundaries in the computational domain were modeled as outflow. The sky was treated as symmetry.

Table 1.
Wind data for the three weather stations

Station	Time (GMT+08:00)	Wind Velocity (m/s)	Wind Direction
Xiqing station	1:00 pm on October 31, 2017	2.8	214° (south-west wind)
Beichen station	1:00 pm on February 25, 2017	2.8	339° (north-north-west wind)
Dongli station	7:00 pm on July 02, 2017	2.7	108° (east-south-east wind)

This investigation used the roughness length method for the ground surfaces to represent roughness elements between the urban configuration and the meteorological stations. The roughness length method incorporates the effects of roughness elements on wind speed and turbulence by using a prescribed aerodynamic roughness z_0 in contrast to the urban terrain, where aerodynamic roughness z_0 is equivalent to the height at which the wind speed theoretically becomes zero. The z_0 value can be found in [38]. In ANSYS Fluent, wall functions with a roughness modification based on the equivalent sand-grain roughness height k_s and the roughness constant C_s can be used to reflect the influence of roughness elements on the urban wind flow field [33]. Therefore, the prescribed aerodynamic roughness z_0 can be defined in ANSYS Fluent after correct conversion to the corresponding k_s and C_s values. This study used the conversion equation from Blocken et al. [1]. Standard wall function was used for the wall surfaces. And the value of y+ was within the range of 30 to 300 for all cases.

$$k_s C_s = 9.793 z_0 \tag{5}$$

Table 2 lists the z_0 values for different terrains [37] and the corresponding k_s and C_s values as converted for this investigation. The legends in Figs. 1 and 3 show the different roughness lengths used for the computational domains according to the building density and building height as determined from a satellite map. Note that when the detailed building structures in Fig. 1(c) were replaced by roughness in the simplified models (Figs. 1(d) to 1(h)), z_0 was set as 1.0 m because the area was highly dense. The surfaces of the buildings in the computational domain were assumed to be non-slip conditions for the wind.

Table 2.
Roughness and case setup for different terrains [1, 38]

Type	z_0 (m)	k_s (m)	C_s
Grassland	0.03	0.5	0.59
Few isolated obstacles	0.05	1.0	0.5
Low crops / Occasional large obstacles	0.1	1.0	1.0
Parkland / Shrubs / Numerous obstacles	0.5	1.0	4.897
Densely distributed mid-rise and high-rise buildings	1.0	1.0	9.793

2.5 Field measurements for CFD validation

Validation of CFD simulations with experimental data is essential. This study calculated wind flow for the university campus with the use of wind information from a meteorological station. For validation purposes, seven HOBO micro weather stations were used to measure the wind velocity magnitude and wind direction on the roofs of four buildings on the campus. The measurement locations were 2 m above the rooftops, and the data was collected from November 6, 2016, to December 31, 2017, as shown in Fig. 5. The building with locations P4 and P5 was our target building. The wind speed and wind direction was measured once every

minute. The measured data was averaged hourly for consistency with hourly data from the meteorological stations. Note that for the wind direction, measured data in one hour may scattered at 0-90° and 270-360° when measured wind was from the north, directly arithmetic mean wind direction will be wrong under such circumstances. Therefore, this investigation processed the wind direction data by plus 360° when the measured data was at the range of 0-90° when wind was from north. Then the revised data will be used to conduct mathematic average. The micro weather stations had a measurement accuracy of ±0.4% for wind speed when it was greater than 0.5 m/s and ±5° for wind direction.

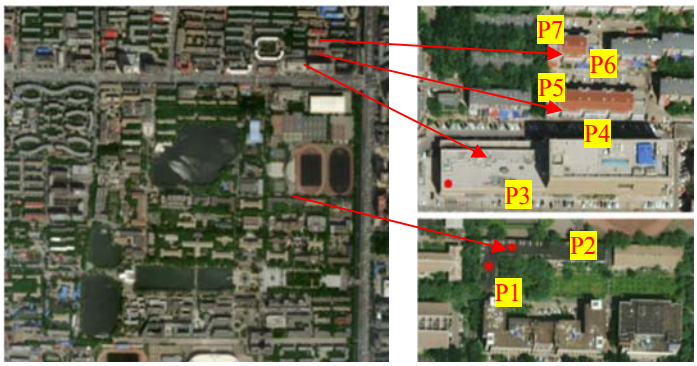

(a) (b)

Fig. 5. Seven measurement positions at a height of 2 m above the rooftops of four buildings on the university campus: (a) building locations and (b) sensor locations.

3. Results

This section describes (1) the comparison of detailed and simplified full-scale geometric models, (2) the comparison of different layers around the target building with Xiqing model, and (3) the comparison of different geometric models for other wind directions.

3.1 Comparison of detailed and simplified full-scale geometric models

This study first compared the detailed full-scale model with the simplified full-scale model in predicting airflow on the university campus, as shown in Fig. 6. The figure depicts the wind flow fields at a height of 2 m above the ground. The average velocity magnitudes over the urban configuration area of interest, as shown in the black box area in Fig. 6, from the detailed full-scale model and simplified full-scale model were 1.28 m/s and 1.35 m/s, respectively. The wind velocity calculated by the simplified model was 5.5% higher than that calculated by the detailed model. In some regions the simplified model had higher velocities in the simplified model than the detailed model. The difference may imply that the roughness length method cannot fully represent the building structures. Although the two models obtained different wind flow fields around buildings located in the upwind direction, such as in the upper wind regions near the bold lines on the left side and at the bottom, this is because the immediate surroundings of these buildings in the upwind direction were excluded in the simplified model, the wind fields were very similar in most areas enclosed by the bold lines, as shown in Fig. 6. Therefore, it can be concluded that the flow field inside the urban configuration was affected primarily by the immediately surrounding building structures rather than the urban architecture between the urban configuration and the meteorological station.

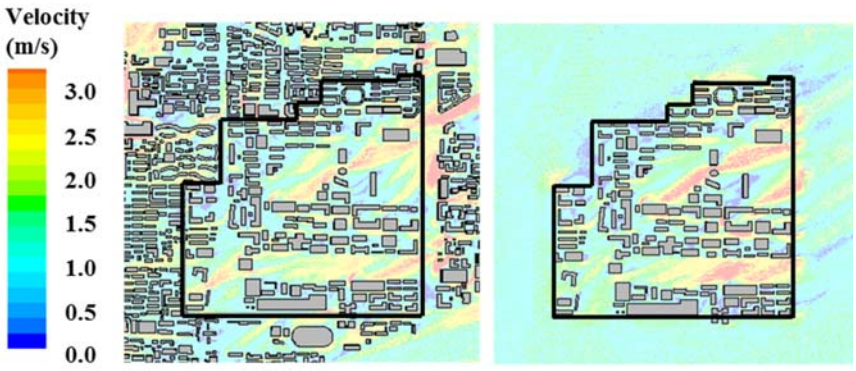

(a) (b)

Fig. 6. Comparison of the wind flow on the university campus as predicted by (a) the detailed full-scale model and (b) the simplified full-scale model.

Fig. 7 compares the simulated wind speed and wind direction with that measured at the rooftop locations in Fig. 5. Our measurements demonstrated that although the hourly wind velocity and wind direction from the meteorological station was the same at all locations, measured data inside the urban configuration varied because the wind was inherently time-dependent. In addition, the location of the HOBO systems (2 m above the roof) might be in the recirculation region above the building so that the measured data would be unstable. Therefore, the error bars of the experimental data represent the variation range of the wind magnitude at the seven measurement locations when the wind information from the meteorological station was the same as that set for the inflow boundary condition. The squares represent the mean wind speed from the experimental data. The results indicate that the computed wind speeds and wind direction from the detailed and simplified full-scale models were within the actual wind variations at most of the positions. The average relative error for the computed wind speed in comparison with the mean experimental data was 31.6% for the detailed full-scale model and 40.8% for the simplified full-scale model. And the average relative error for the computed wind direction in comparison with the mean experimental data was 9.4% and 10.7% for the detailed full-scale model and the simplified full-scale model, respectively. Neither model considered the trees around the buildings, only taking into account the influence of the trees by means of the roughness length of 0.03 m inside the urban configuration, as shown in Fig. 1. In addition, there were differences between the geometric model and the actual building structures even inside the urban configuration. Therefore, we considered the computed results acceptable for such a complex case. The results obtained by the simplified full-scale model were very close to those from the detailed full-scale model, and thus the simplified model could be used to calculate wind distribution in an urban configuration.

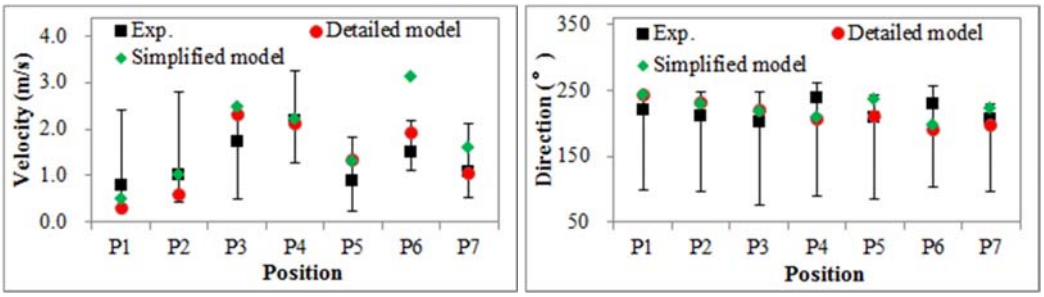

(a) (b)

Fig. 7. Comparison of the wind speed simulated by the detailed and simplified full-scale models with that measured at seven locations on building rooftops inside the urban configuration: (a) wind velocity and (b) wind direction.

This study also compared the computing time required by the two CFD models. All the simulations were performed on a workstation with 24 cores and 128 Gb memory. The computing times for the detailed and simplified full-scale models were 41.8 h and 28.7 h, respectively. The simplified full-scale model used a grid number that was only 69% of that in the detailed full-scale model. Thus, the simplified model can reduce computing time by at least one third. In addition, the effort required to construct the geometric model was much smaller for the simplified model, because it did not require detailed building information outside the urban configuration concerned. Therefore, the simplified full-scale model is a better choice for numerical simulation of an urban wind environment.

3.2 Comparison of different layers around the target building

After validating the method used to represent the intermediate terrain with roughness, this investigation studied the influence of surrounding layers on the wind flow around the target building. Next, the performance of the other five geometrical models with different surrounding layers for predicting the wind speed and static pressure around the target building was explored. The prediction by the simplified full-scale model was used as the baseline for comparison. All the models used the same wind velocity profiles from the meteorological station as the inlet boundary conditions and the same roughness length on the ground surface without building details.

Fig. 8 depicts the wind flow around the target building (the black rectangle) as predicted by the models at a height of 2 m above the ground. The wind flow field computed by the R = 0 model was very different from the fields computed by the other models. The R = 0 model could not take into account the effect of the surrounding buildings on the wind direction and velocity magnitude around the target building. The wind velocities around the building predicted by the R = L and R = 2L models were larger than the velocity predicted by the R = 0 model because of the channeling effect generated by the adjacent buildings. With the inclusion of the surrounding buildings in the R = 3L and R = 4L models, the wind speed decreased because of blockage by the buildings in the outer layer. The wind flow fields obtained by the R = 3L and R = 4L models were similar to that obtained by the simplified full-scale model (or TJU model, as shown in Figs. 8-12), which was considered to be the most accurate because it took into account the large, detailed building structures. The surrounding area incorporated by the R = 3L model seemed to be the minimum required for obtaining acceptable wind flow around the building in the CFD simulation.

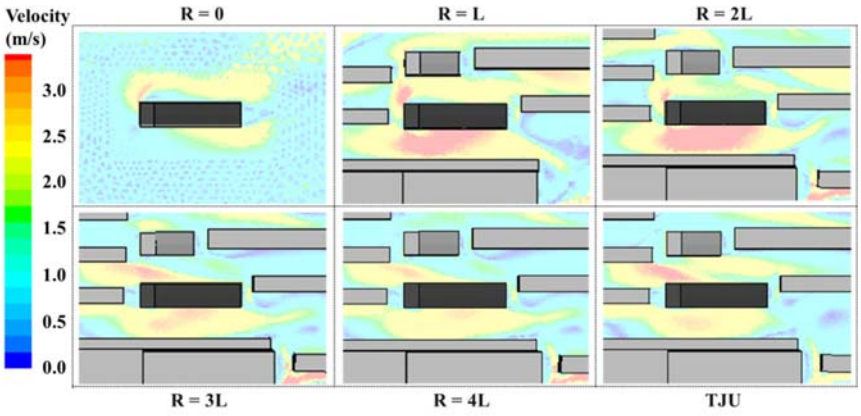

Fig. 8. Comparison of the wind flow around the target building as predicted by the six models.

Fig. 9 compares the static pressure distributions around the target building as computed by the six models. Since the wind struck the target building directly in the R = 0 model, the pressure distribution in the windward direction was the highest, as shown in Fig. 8. Because of the very different airflow pattern in the leeward direction, the R = 0 model also predicted a very different pressure distribution, as shown in Fig. 9(b). As an increasing number of surrounding buildings were included in the simulations, the pressure distributions gradually became similar to those produced by the TJU model. Again, the results indicate that surrounding area incorporated by the R = 3L model seemed to be the minimum necessary for obtaining acceptable pressure distributions around the building.

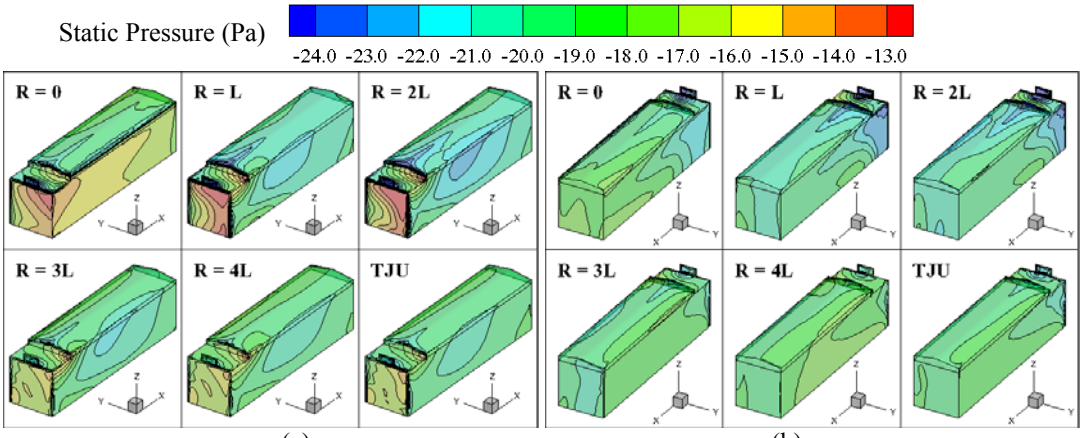

Fig. 9. Comparison of the static pressure distributions around the building as simulated by the six models: (a) in the windward region and (b) in the leeward region.

Fig. 10 further compares the wind velocity at P4 and P5, which were located on the roof of the target building, and the average static pressure difference in the windward region (south and west walls) and leeward region (north and east walls) as computed by the six models. We have not included other data because the R = 0 model did not incorporate information about the other buildings. Because of the channeling effect created by the surrounding buildings, the wind velocity at P5 increased from the R = 0 to the R = L model. The velocity magnitude at the two locations then decreased with the increase in the number of surrounding buildings and gradually approached the experimental data (mean wind speed measured at P4 and P5) from the R = 3L to R = 4L to TJU model. The velocity magnitude decreased with the increase in the number of buildings around the target building. When $R \geq 3L$, the results were the same as those of the TJU model, and therefore the R = 3L model seems sufficient. The pressure difference (ΔP) of the target building decreased from 6.9 Pa in the R = 0 model to 5.5 Pa in the R = L model. This is because the target building was no longer struck directly by the approaching wind. The pressure difference decreased with the increase in the number of the surrounding buildings and gradually became stable at 2.3 Pa when $R \geqslant 3L$, because of the sheltering effect of the surrounding buildings. Both the velocity magnitude and pressure difference decreased with the increase in the number of buildings around the target building. When $R \geqslant 3L$, the results were the same as the TJU model, and therefore the R = 3L model again seems sufficient.

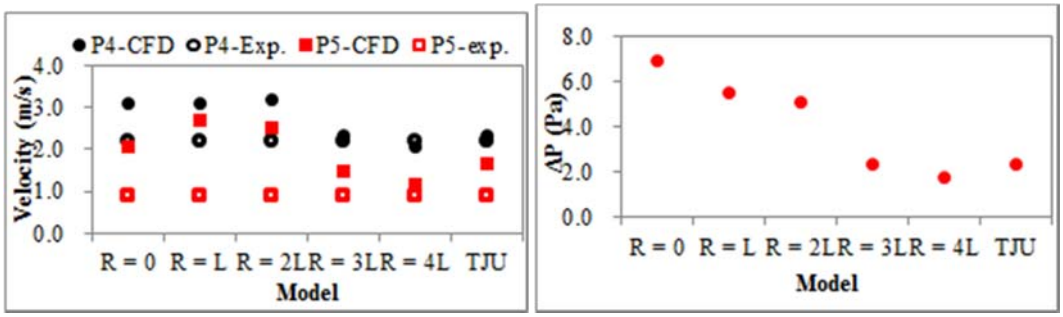

(a) (b)

Fig. 10. Comparison of (a) wind speed and (b) static pressure difference as simulated by the six models.

3.3 Comparison of different geometric models for other wind directions

Sections 3.1 and 3.2 discussed the performance of the roughness method in representing the immediate terrain, and the influence of surrounding layers of buildings on the wind flow around the target building from one wind direction. In order to verify that the results are sufficiently universal, this study also performed simulations for the other two wind directions.

Fig. 11 compares the simulated wind speed and wind direction on the rooftops of the buildings on the campus with the measured data for the other two simplified full-scale models shown in Figs. 3(b) and 3(c). Again, the error bars of the experimental data represent the variation range of the wind magnitude at the seven measurement locations when the wind information from the meteorological stations was the same as that set for the inflow boundary conditions. The squares represent the mean wind speed from the experimental data. The results show that the wind speeds computed by the simplified full-scale models for the Beichen station (Fig. 11(a) and Fig. 11(b)) and Dongli station (Fig. 11(c) and Fig. 11(d)) were within the actual wind speed and wind direction variations at most locations except for P4 in Fig. 11(d). This is probably because P4 was located in the vortex zone due to the block of the pitched roof, as shown in Fig. 9, on the east side of the target building. Therefore, it was difficult to accurately calculate the wind direction as well as wind speed. The average relative errors of computed wind speed compared with the mean experimental data for the two simplified full-scale models were 26.0% and 22.6%, respectively. And the average relative errors of computed wind direction compared with the mean experimental data for the two simplified full-scale models were 3.5% and 31.3%, respectively. Because of the simplifications of the geometric models, we considered the computed results acceptable for such complex cases. These two simulations confirmed the results shown in Section 3.1, i.e., that the simplified full-scale model can be used for numerical simulation of an urban wind environment.

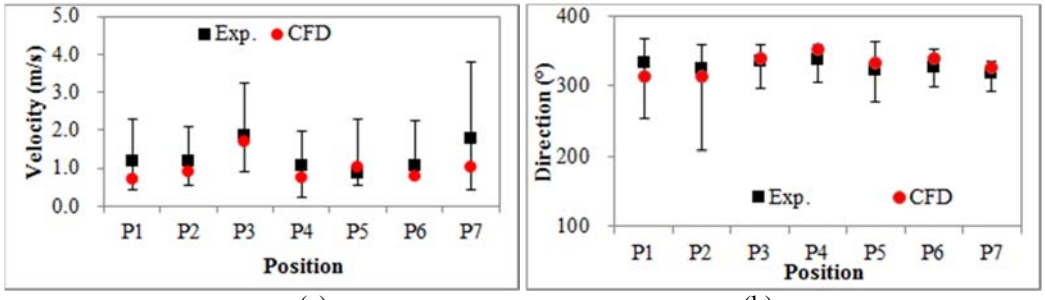

(a) (b)

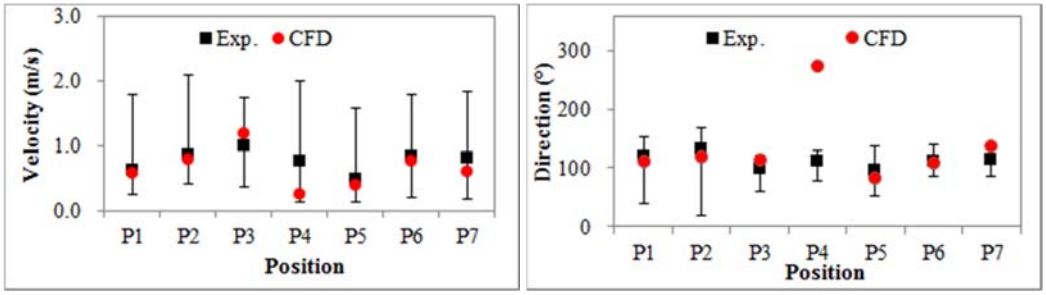

(c) (d)

Fig. 11. Comparison of the wind speed and wind direction as simulated by the simplified full-scale models with that measured at seven locations on building rooftops in the urban configuration: (a) wind speed computed by Beichen model, (b) wind directioncomputed by Beichen model, (c) wind speed computed by Dongli model, and (d) wind direction computed by Dongli model.

Fig. 12 further compares the velocity at P4 and P5, which were located on the rooftop of the target building, as computed by the different models with different surrounding layers. Fig. 9 shows the sheltering effect of the baffle on the roof of the target building. The wind velocity at P4 and P5 decreased from the R = 0 model to the R = L model because these points were located in the recirculation zone in the Beichen model, as shown in Fig. 12(a). As the number of surrounding buildings increased, the velocity magnitude at the two locations increased because of the change in wind direction and velocity magnitude around the building, and gradually approached the experimental data from the R = 3L to R = 4L to TJU model. Fig. 9 also indicates that the pitched roof on the east side of the target building may block most wind from the southeast for the Dongli model. Fig. 12(b) shows that the wind velocity at P4 and P5 did not change greatly from the R = 0 to the R = 4L model. A comparison of the wind flow and static pressure distributions around the target building with different surrounding layers again shows that the R $\geqslant$ 3L models performed as well as the TJU model.

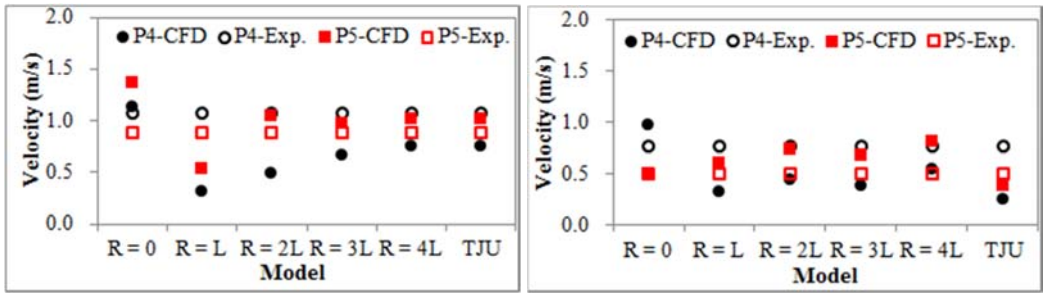

(a) (b)

Fig. 12. Comparison of the wind speed simulated by the simplified full-scale models with that measured at seven locations on building rooftops in the urban configuration: (a) Beichen model and (b) Dongli model.

4. Discussion

This investigation further compared the region where surrounding buildings should be explicitly constructed according to our investigation with the other two earlier guidelines from Tominaga et al. [10] and Tong et al. [31]. The comparison was performed using the same urban configuration. The region from Tominaga et al. [10] was the smallest, as shown in Fig. 13(a). They suggested using the height of the target building as radius to cover surrounding buildings. However, for the urban configuration used in this study, the target building exhibited a low height of 16 m but a large length of 65 m. The region from Tong et al. [31] was the largest, as shown in Fig. 13(b). But it was difficult to define surrounding

layers based on building blocks because buildings were densely distributed in some directions while sparsely in other directions. This investigation chose the maximum dimension of the building as a scale in the radial direction to cover surrounding buildings. The results of this investigation may be more practical for use.

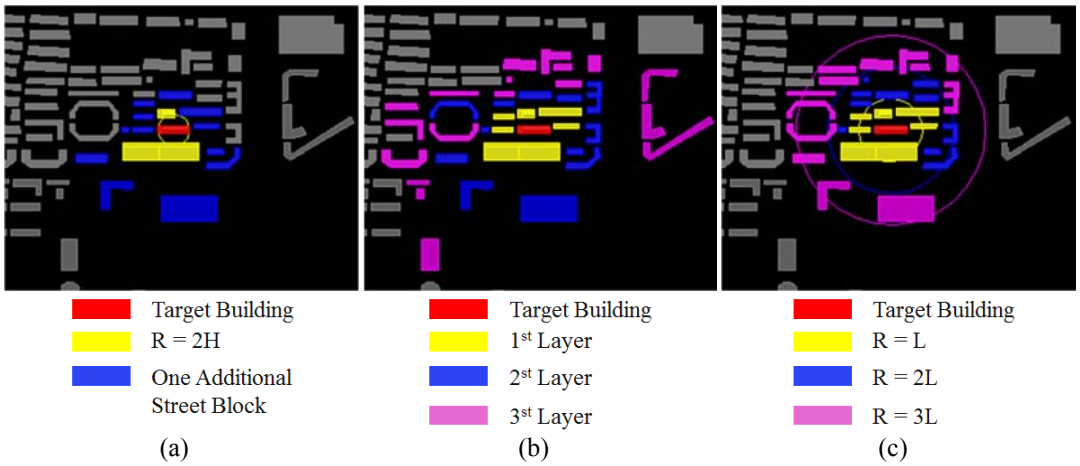

Fig. 13. Comparison of the region where surrounding buildings should be explicitly constructed according to: (a) Tominaga et al. [10], (b) Tong et al. [31] and (c) our investigation.

The full-scale model performed quite well for the complex cases presented in this study. However, the model had several limitations:

- The location of the HOBO systems (2 m above the roof) might be in the recirculation region above the building. Therefore it might be difficult to obtain a good agreement between the simulation results and the measurement data.
- The detailed full-scale geometrical model was established with the aid of a satellite image because no geometric models were publicly available. The roughness partition of the simplified full-scale model was based on this image. The model used approximations that may have affected the wind profiles. We were unable to estimate the errors that may have resulted.
- This study used a realizable k-ε model to simulate the urban wind flow under steady-state conditions. However, wind constantly changes in direction and magnitude. Should a transient simulation method be used, it could improve the accuracy but would significantly increase the computing costs.
- There were only three weather stations located close to the university campus. In actual practice, wind could flow into the urban configuration from all directions. Can we reliably use wind information from the three stations for calculating airflow on the university campus? If there were only one weather station in the city, could we use the wind information from this station as the boundary condition if the wind came from the opposite direction?

5. Conclusions

This investigation conducted CFD simulations of the wind environment in an urban configuration to identify a suitable method for simulating intermediate terrain with the use of roughness length. Next, this investigation conducted CFD simulations of the wind environment around a building to identify the minimum size of the surrounding area, with detailed building structures, that should be included in the geometric model. The study led to the following conclusions:

- The velocity flow fields obtained with the detailed and simplified full-scale models were very similar. The mean wind velocity computed by the simplified model was 5.5% higher than that computed by the detailed model inside the urban configuration. This may imply that the roughness length method cannot fully represent the building structures, but the error was not significant.
- The simplified full-scale model used only 69% of the grid number used by the detailed full-scale model. Thus, the simplified model can reduce the computing time by at least one-third, as well as the effort required to construct the geometric model.
- The airflow and pressure distributions around the target building computed with the use of only the building and different roughness lengths for the surroundings (the R = 0 model) did not generate acceptable results. By using the maximum dimension of the building, L, as the scale, this study found that the region within at least a 3L radius of the building should be simulated with detailed building structures in order to obtain sufficiently accurate wind flow and pressure distributions around the building.

Acknowledgement

The research presented in this paper was partially supported by the National Key R&D Program of the Ministry of Science and Technology, China, on "Green Buildings and Building Industrialization" through Grant No. 2016YFC0700500 and by the National Natural Science Foundation of China through Grant No. 51678395.

References

[1] Blocken, B., Stathopoulos T., Carmeliet J. CFD simulation of the atmospheric boundary layer: Wall function problems. Atmospheric Environment, 41 (2007) 238-252.

[2] Blocken, B. Computational Fluid Dynamics for urban physics: Importance, scales, possibilities, limitations and ten tips and tricks towards accurate and reliable simulations. Building and Environment, 91(2015) 219-245.

[3] Razak, AA., Hagishima, A., Salim, SAZS. Progress in wind environment and outdoor air ventilation at pedestrian level in urban area. Applied Mechanics & Materials, 819 (2016) 236-240.

[4] Yukio, T., and Ryuichiro, Y. Advanced Environmental Wind Engineering. Japan. 2016.

[5] Willemsen, E., and Wisse, JA. Design for wind comfort in the Netherlands: Procedures, criteria and open research issues. Journal of Wind Engineering and Industrial Aerodynamics, 95 (2007) 1541-1550.

[6] Chen, Q. "Chapter 7: Design of natural ventilation with CFD," Sustainable Urban Housing in China, Edited by L.R. Glicksman and J. Lin, Springer. 2006, pp. 116-123.

[7] Ramponi, R., Blocken, B., Coo, LBD., et al. CFD simulation of outdoor ventilation of generic urban configurations with different urban densities and equal and unequal street widths. Building and Environment, 92 (2015) 152-166.

[8] Jin, M., Zuo, W., and Chen, Q. Simulating natural ventilation in and around buildings by fast fluid dynamics. Numerical Heat Transfer, Part A: Applications, 64(4) (2013) 273-289

[9] Liu, S., Liu, J., Yang, Q., et al. Coupled simulation of natural ventilation and daylighting for a residential community design. Energy and Buildings, 68 (2014) 686-695.

[10] Tominaga, Y., Mochida, A., Yoshie, R., et al. AIJ guidelines for practical applications of CFD to pedestrian wind environment around buildings. Journal of Wind Engineering and Industrial Aerodynamics, 96 (2008) 1749-1761.

[11] Hang, J., and Li, Y. Wind conditions in idealized building clusters: Macroscopic simulations using a porous turbulence model. Boundary-Layer Meteorology, 136 (2010) 129-159.

[12] Britter, RE., Hanna, SR. Flow and dispersion in urban areas. Annual Review of Fluid Mechanics, 35 (2003) 469-496.

[13] Liu, H., Zhang, B., Sang, J., et al. A laboratory simulation of plume dispersion in stratified atmospheres over complex terrain. Journal of Wind Engineering & Industrial Aerodynamics, 89(1) (2001) 1–15.

[14] Tong, H., Walton, A., Sang, J., et al. Numerical simulation of the urban boundary layer over the complex terrain of Hong Kong. Atmospheric Environment, 39(19) (2005) 3549-3563

[15] Martilli, A., and Santiago, JL. CFD simulation of airflow over a regular array of cubes. Part II: Analysis of spatial average properties. Boundary-Layer Meteorology, 122(3) (2007) 635-654.

[16] Santiago, JL., Martilli, A., and Martin, F. CFD simulation of airflow over a regular array of cubes. Part I: Three-dimensional simulation of the flow and validation with wind-tunnel measurements. Boundary-Layer Meteorology, 122(3) (2007) 609-634.
[17] Liu S., Pan W., Zhang H., et al. CFD simulations of wind distribution in an urban community with a full-scale geometrical model. Building and Environment, 117(2017) 11-23.
[18] Badger, J., Hahmann, AN., Volker, PJH., et al. Wind resource mapping in Ethiopia : mesoscale wind modeling report (English). Energy Sector Management Assistance Program. Washington, D.C.: World Bank Group. 2016.
[19] Coceal, O., and Belcher, SE. A canopy model of mean winds through urban areas. Quarterly Journal of Royal Meteorological Society, 130 (2004) 1349-1372.
[20] Sabatino, SD., Solazzo, E., and Paradisi, P. A simple model for spatially-averaged wind profiles within and above an urban canopy. Boundary-Layer Meteorology, 127 (2008) 131-151.
[21] Peng, Z., and Sun, J. Characteristics of the drag coefficient in the roughness sublayer over a complex urban surface. Boundary-Layer Meteorology, 153 (2014) 569-580.
[22] Crago, RD., Okello, W., and Jasinski, MF. Equations for the drag force and aerodynamic roughness length of urban areas with random building heights. Boundary-Layer Meteorology, 145 (2012) 423-437.
[23] Skote, M., Sandberg, M., Westerberg, U., et al. Numerical and experimental studies of wind environment in an urban morphology. Atmospheric Environment, 39 (2005) 6147-6158.
[24] Kuwahara, F., Yamane, I., and Nakayama, A. Large eddy simulation of turbulent flow in porous media. International Communications in Heat and Mass Transfer, 33(4) (2006) 411-418.
[25] Ng, E., Yuan, C., Chen L., et al. Improving the wind environment in high-density cities by understanding urban morphology and surface roughness: A study in Hong Kong. Landscape and Urban Planning, 101 (2011) 59-74.
[26] Kim, BG., Lee, C., Joo, S., et al. Estimation of roughness parameters within sparse urban-like obstacle arrays. Boundary-Layer Meteorology, 139 (2011) 457-485.
[27] Cao, M., and Lin, Z. Impact of urban surface roughness length parameterization scheme on urban atmospheric environment simulation. Journal of Applied Mathematics, 12(2) (2014) 155-175.
[28] Mara TG., Ho TCE., and Isyumov N. 2012. Interference and Influence of Nearby Buildings: A Discussion of the Design Approach. Structures Congress 2012 © ASCE 2012.
[29] Asfour, OS. Prediction of wind environment in different grouping patterns of housing blocks. Energy and Buildings, 42 (2010) 2061-2069.
[30] Hooff, TV., and Blocken, B. On the effect of wind direction and urban surroundings on natural ventilation of a large semi-enclosed stadium. Computers & Fluids, 39 (2010) 1146-1155.
[31] Tong, Z., Chen, Y., and Malkawi A. Defining the Influence Region in neighborhood-scale CFD simulations for natural ventilation design. Applied Energy, 182(2016) 625-633.
[32] http://data.cma.cn/
[33] ANSYS Inc.. ANSYS Fluent 14.0 User's Guide. ANSYS Inc. Southpointe. 2011.
[34] Shih, TH., Liou, WW., Shabbir, A., et al. A new k-ε eddy-viscosity model for high Reynolds number turbulent flows – Model development and validation. Comput Fluids, 24(3)(1995) 227-38.
[35] Blocken, B., and Persoon, J. Pedestrian wind comfort around a large football stadium in an urban environment: CFD simulation, validation and application of the new Dutch wind nuisance standard. J. Wind Eng. Ind. Aerodyn., 97(2009) 255-270.
[36] Richards, PJ., Hoxey, RP.. Appropriate boundary conditions for computational wind engineering models using the k-ε turbulence model. J. Wind Eng. Ind. Aerodyn. 46&47(1993) 145-153.
[37] Gu, J. Dictionary of atmospheric science. Beijing, China Meteorological Press, (1994) 156.
[38] Wieringa, J. Updating the Davenport roughness classification. Journal of Wind Engineering and Industrial Aerodynamics, 41(1-3) (1992) 357-368.